A study of source spectrum, site amplification functions, response spectra, Fourier spectra, and peak ground accelerations from the strong ground motion data of the 1991 Uttarkashi earthquake

V. Sriram and K. N. Khattri

Wadia Institute of Himalayan Geology, Dehradun 248 001, India

The strong ground motions recorded during the Uttarkashi earthquake of 1991 (Ms 7) are analysed for the estimation of source spectrum, site amplification function, decay with distance of peak acceleration and Fourier and Response spectral characteristics. The source spectrum is found to be complex and requires dual corner frequency Brune model to represent it. The high frequency portion of the spectrum, showing the roughness of faulting corresponds to a stress drop of 40 bars, whereas the intermediate to low frequency portion of the source spectrum, related to the overall slip over the fault plane, has a stress drop of 31 bars. The stations in the distance range of 50 km and above show a significant amplification at higher frequencies and the nearer ones like Tehri, Bhatwari and Barkot have amplifications at lower frequencies. The estimate of the site amplification shows an amplification of the order of 3 at some sites. At Tehri the amplification in horizontal components is about 2.5 for the period range of 1.0 to 2.5 s.

THE analysis of near-field of the ground motion gives an opportunity to look into the source processes in finer detail and in establishing relations describing the peak ground motion and response spectra as a function of distance and magnitude in the affected region. These relations are of paramount importance in assessing hazard for the design of engineered structures. The Himalayan region, which has a high seismic hazard potential, has very few strong motion recording sites. The Uttarkashi earthquake of 1991 (Ms 7.0) is the first large earthquake to be recorded at short distances in the Garhwal Himalaya and has provided important database for the appraisal of strong motion expected from a future earthquake in the region. The earthquake inflicted heavy damage, claimed over 2000 lives, left 5000 injured and rendered 10,000 homeless. The economic loss was estimated at Rs 400 crores[1]. The earthquake occurred at 3:45 (IST) in the night hours on account of which the death toll was high. This region was also the site of an earlier earthquake of similar magnitude in 1903 (ref. 2).

We examine here this data set to estimate and model the source spectrum, the site amplification functions, the rate of decay of peak acceleration with distance and the characteristics of the Fourier and the response spectra. We also compare the peak accelerations recorded by structural response recorders and strong motion recorders at some sites.

Seismic regime

Earthquakes in the Himalaya are fed by strain accumulation in the region, which is the boundary between the Indian and the Eurasian plates, that converge at a rate of about 55 mm per year[3]. The great earthquakes that are the principal means of relieving strain occur by thrusting on a sub-horizontal detachment surface[4]. The depth of this detachment surface is approximately 20 km at its northern end. The great earthquakes in the Himalaya in the last 100 years have ruptured sections of the plate boundary in lengths of 250 to 350 km, leaving sectors in between that have not ruptured in the last several centuries[5].

The 1991 Uttarkashi earthquake occurred at the western end of the central gap defined by Khattri and Tyagi[2,5]. This end of the seismic gap is bordered by the eastern edge of the rupture that occurred in the great gap filling 1905 Kangra earthquake[6].

Earthquake parameters

Preferred parameters of the 1991 earthquake estimated from teleseismic analysis are as follows. Estimation of

the location also utilized data from the regional and local stations of India Meteorological of Department (IMD).

Origin time: 21:23:14.38 (GMT)
Location: 30.75°N; 78.86°E; H = 12 km
$Mo = 1.8 \times 10^{26}$ dyne-cm
Ms = 7.0, Mw = 6.8, mb = 6.5
NP1: strike 317°; dip 14°; slip 115°
NP2: 112°; 78°; 84°

The nodal plane 1 dipping towards the NW at a low angle is the preferred fault plane as it is consistent with the distribution of aftershocks as well as with the geodynamic model of the region.

The epicenter and the aftershock zone defining the fault area of this earthquake lies in the crystalline rock province of the High Himalaya[7]. The Main Central Thrust follows just on the south of the surface projection of the fault trace (Figure 1). The focal mechanism of the event is also shown in the figure.

Strong motion accelerograms

Strong motion station locations are shown in Figure 1. The figure also shows the surface traces of the Main Central Thrust and the Main Boundary Thrust of Himalaya. Except for Bhatwari, which is situated in the central crystalline province of the Higher Himalaya, the rest of the stations are located in the meta-sedimentary province of the Lesser Himalaya. While Bhatwari is located near the western edge of the estimated position of the fault plane[8], the remaining stations are located quite away from it. The stations may also be grouped in terms of azimuth with respect to the direction of the rupture propagation and the smallest distance from the surface projection of the fault edge. Thus, Bhatwari, Uttarkashi, Barkot, Purola and Koti lie in line with the forward direction of rupture propagation; Ghansiali, Tehri, Srinagar, Rudraprayag and Koteshwar lie in the direction of slip and have an oblique angle with the rupture propagation direction; Karnaprayag, Kosani and Almora are towards a direction away from the direction of rupture propagation. Therefore, on account of rupture propagation the ground motion amplitudes at the first group of stations would be expected to be enhanced, and their frequencies increased due to Doppler shift. On the other hand, the wave amplitudes and frequencies should be reduced for the last group of stations in the rear, while for the second group of stations it should be between the

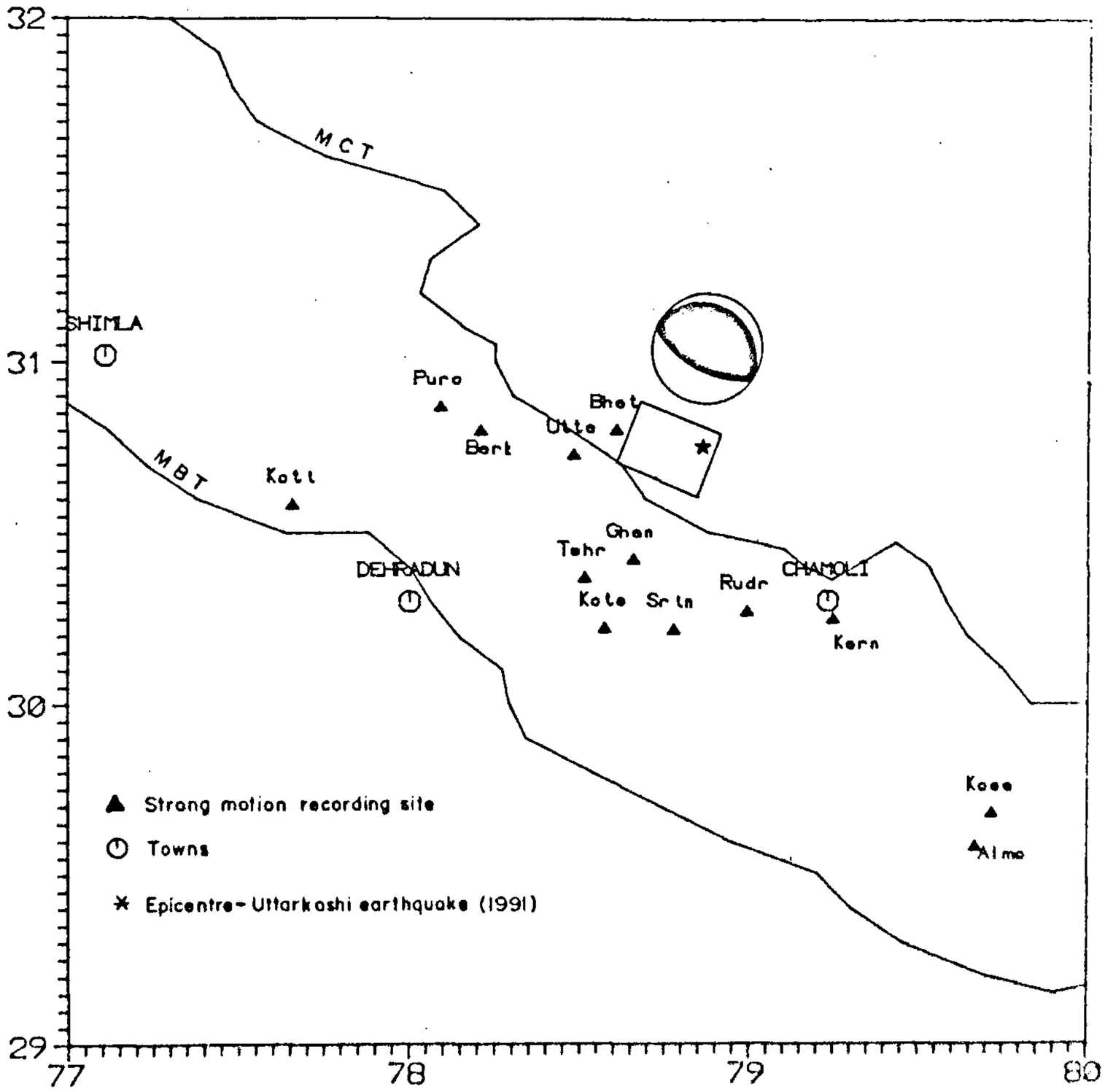

Figure 1. Location of Uttarkashi earthquake (star) and its fault plan solution are shown. The stations are shown as triangles. MBT, Main Boundary Thrust; MCT, Main Central Thrust. The rectangle shows the estimated fault area.

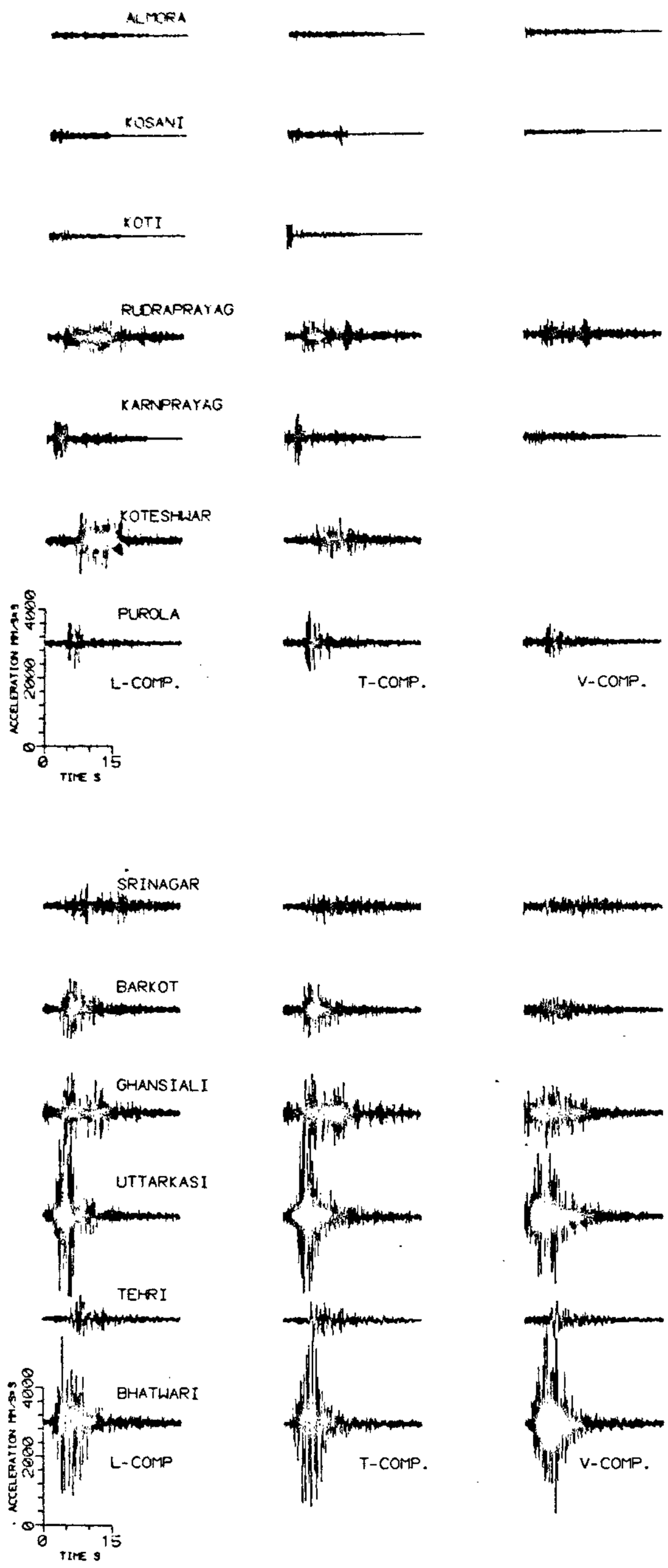

Figure 2. Accelerograms recorded during the Uttarkashi earthquake.

above two ranges. For stations up to a distance of about 60 km, the ground motions are dominated by the direct waves. Beyond this distance the post-critical reflections from Moho and layers within the crust, and *Lg* phases will contribute significantly to the ground motion. There will also be spreading over time of the waves in this distance range.[9]

The strong motion waveforms are shown in Figure 2. These recordings are triggered at some threshold and show the arrival of shear waves starting from where the amplitudes suddenly become large. The data is filtered through a band pass filter (0.17–0.20; 22.0–27.0 Hz). The distances of the stations from the fault edge and the peak acceleration, velocities and displacements are given in Table 1.

The recordings at Bhatwari and Uttarkashi, the two nearest stations show the highest levels of peak accelerations, namely 0.27 g and 0.31 g. We note that another accelerograph at Uttarkashi recorded a peak acceleration of 0.53 g (ref. 10). The waveforms show two bursts of energy spaced by about 2 s. The high frequency signals are overriding the large impulses which have a period of about 1 s. An inversion for the source slip function for this earthquake has mapped several asperities over the fault plane. The two impulses in the records are indicative of the rupturing of the two larger asperities of the fault plane. The durations of strong shaking, defined by a threshold of 0.05 g are approximately 9 s at Bhatwari and 8 s at Uttarkashi (Table 1). The larger peak acceleration observed at Uttarkashi which is at a distance of 10 km as compared to about ~1 km for Bhatwari may be due to local site geology. The Uttarkashi station is in Lesser Himalaya having softer meta-sedimentary rocks and may have a top low velocity layer, whereas Bhatwari is located over crystallines and may lack a significantly thick low velocity top layer. Another factor is that Bhatwari is expected to have a lower amplitude than Uttarkashi on account of the point source radiation pattern of the earthquake.

The stations at Barkot and Purola which are at distances of 32 and 43 km respectively have a relatively richer component of the higher frequencies in the accelerograms as compared to the observed ones at Bhatwari and Uttarkashi. This is surprising as the higher frequencies are expected to attenuate faster than the lower frequencies. The peak accelerations and duration of shacking at these stations have dropped to 0.1 g; 4 s and 0.1 g; 2 s respectively.

The accelerograms at Ghansiali, Tehri and Koteshwar are in the distance range of 26 to 49 km. They record peak accelerations of 0.14 g, 0.07 g and 0.1 g respectively. The durations are 8 s, 2.5 s and 9 s respectively. The accelerograms at Ghansiali and Koteshwar are richer in the high frequencies. There is significant ringing at Koteshwar. The long duration of the signal at this station is on this account. The signals of lower frequencies are especially prominent at Tehri.

The next group of stations are at distances of 45 to 54 km, namely Rudraprayag, Srinagar and Karnprayag

Table 1. Peak ground acceleration S and duration of strong shaking recorded during the Uttarkashi earthquake

Station name code	Epicentral distance (km)	Distance from surface proj. of fault (km)	A_{max} L cm/s^2	A_{max} T cm/s^2	A_{max} V cm/s^2	Duration of strong shaking (s)
Bhatwari (Bhat)	25.0	0.0	248.37	241.89	288.78	9.0
Uttarkashi (Utta)	36.0	10.0	237.27	303.99	192.62	8.0
Ghansiali (Ghan)	41.0	26.0	115.59	114.89	99.23	8.0
Tehri (Tehr)	54.0	39.0	71.41	61.13	57.82	2.5
Barkot (Bark)	63.0	32.0	93.18	80.47	43.65	4.0
Srinagar (Srin)	60.0	45.0	65.44	49.45	33.09	1.5
Rudraprayag (Rudr)	54.0	44.0	52.29	50.76	44.13	9.0
Koteshwar (Kote)	65.0	49.0	98.85	65.23	74.34	9.0
Karanprayag (Karn)	67.0	54.0	60.99	77.35	25.96	2.5
Purola (Puro)	75.0	43.0	73.95	91.68	51.74	2.0
Koti (Koti)	116.0	89.0	20.64	40.95	14.25	1.5
Kosani (Kosa)	144.0	144.0	28.34	31.50	11.04	1.0
Almora (Almo)	150.0	150.0	17.41	21.02	18.44	0.5

which are located in the opposite direction of rupture propagation. The peak accelerations and duration of group shaking are 0.06 g, 9 s; 0.06 g, 1.5 s; and 0.08 g, 2.5 s respectively. The records at Rudraprayag and Srinagar display a considerable amount of high frequencies. Karnaprayag has lower frequency content. The long duration observed at Rudraprayag appears to be a case of ringing, perhaps in a shallow low velocity layer. The peak accelerations at Srinagar and Rudraprayag are lower as compared to at Purola. This is interpreted to be due to the directivity effect of the rupture propagation. These stations are at similar distances, but Purola is in the direction of rupture propagation while the other two stations are in the opposite direction.

The remaining three stations are Koti, Kosani and Almora at distances greater than 100 km. The ground motions at these sites will be dominated by the Lg phase. The acceleration levels are quite small and of relatively lower frequencies.

The wave packets carrying most of the energy at the stations in the distance range of 30 to 55 km are more dispersed than at Bhatwari and Uttarkashi. The higher frequency content is likely to be due to the P waves coming in as wide angle reflections from the top of the basement which is expected at a depth of about 17 km (ref. 2). The direction for such waves is near maximum for the radiation pattern of the earthquake.

Attenuation of peak ground acceleration

The values of the peak ground acceleration at various stations are plotted as a function of epicentral distance in Figure 3. The decay is faster at distances less than 50 km and steady after that. The attenuation relations for peak ground acceleration with epicentral distance[11–14], are also shown for comparison. McGuire's relation overpredicts the expected ground acceleration

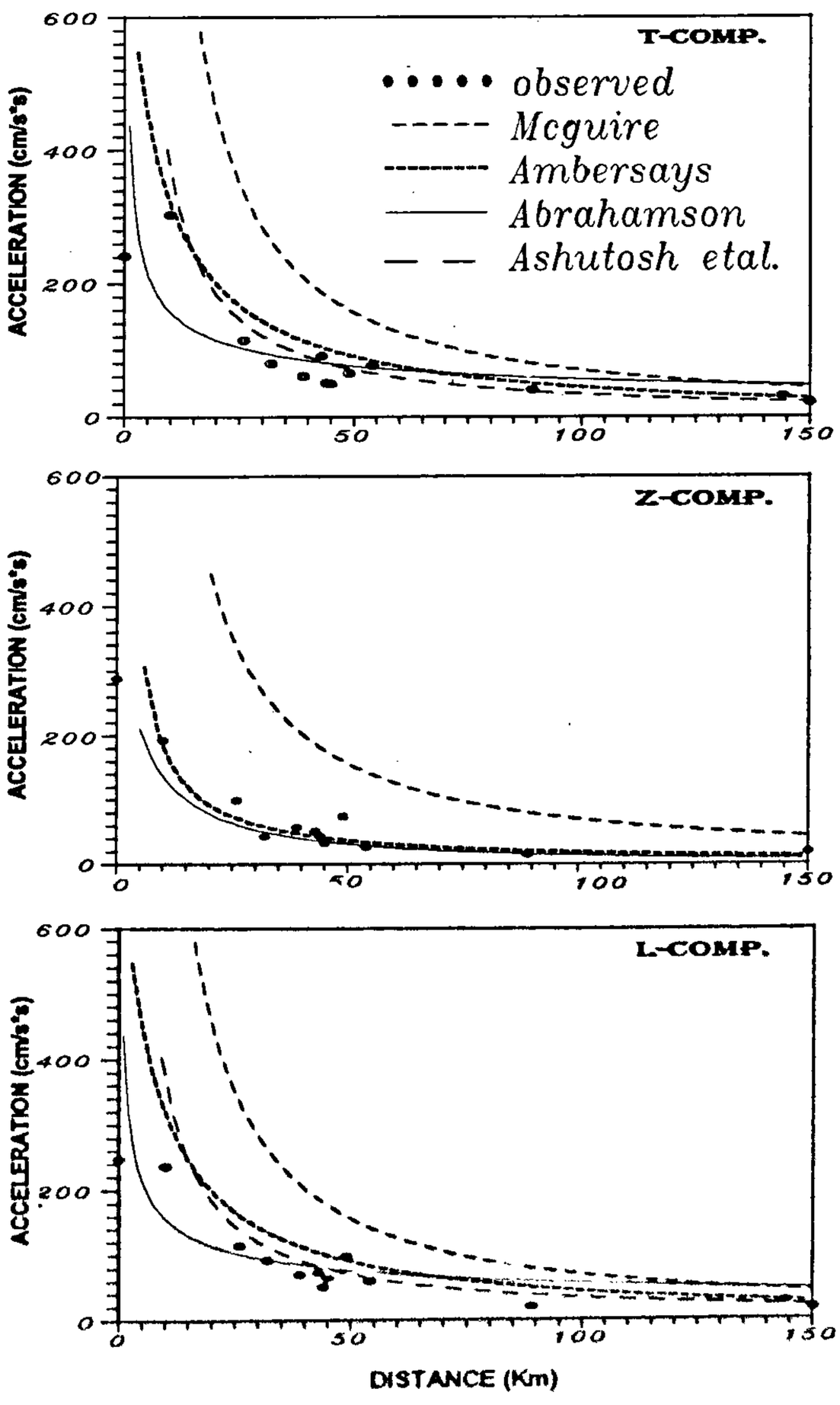

Figure 3. Dependence of peak ground acceleration with distance. See text for regression.

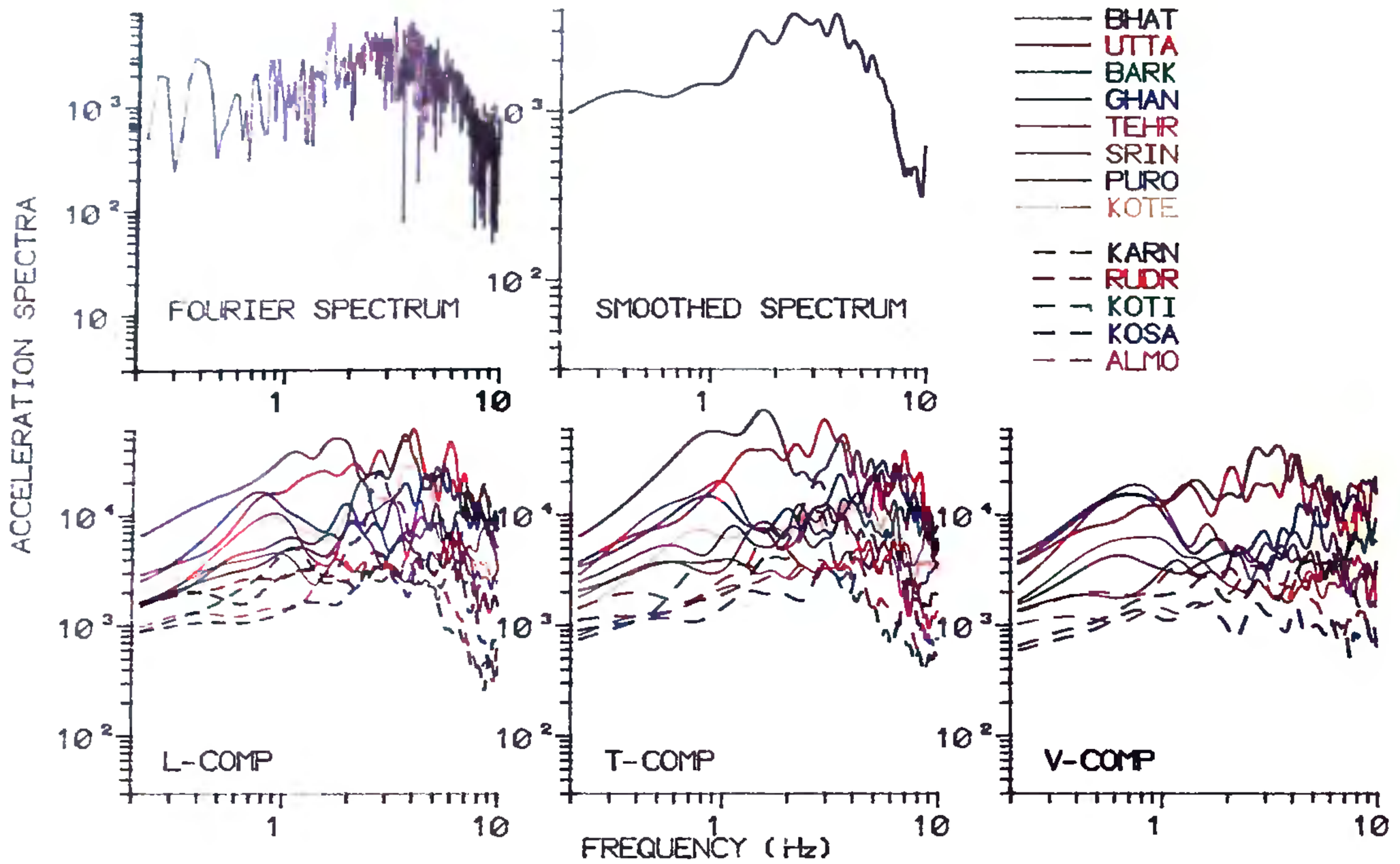

Figure 4. Fourier spectrum of the accelerograms. The top panel shows the spectrum obtained using FFT and the corresponding smoothed spectrum for the station ALMO (L-Comp). The bottom panel shows all the smoothed spectra.

in all the three components. Ambrasey's relation which is based on the European data set matches the observed peaks in vertical component. For the horizontal components the match is good for distances greater than 50 km. Abrahamson and coworker's relation based on data from different parts of the world, shows a better fit in the vertical component but overpredicts at short distances for the horizontal components[13]. Ashutosh *et al.*[14] used data from various Himalayan earthquakes (including this event) in their regression for attenuation relation. This relation gives a better match at short distances up to 50 km but the predicted peak accelerations are higher than the observed ones for the distant stations. This could be due to the inclusion of data set from the Shillong Massif region of NE Himalaya where some of the earthquakes are of intermediate depth and the observed attenuation is unusually lower than in other parts of Himalaya. The inadequacies in representing the decay of peak acceleration by these regression relations emphasizes the need for a localized database to model the attenuation properties of the region.

Fourier spectra

The Fourier spectra of all the recordings have been estimated using Tukey–Hamming technique. Figure 4 shows a spectrum obtained using the fast Fourier transform algorithm. This estimate is quite rough. The corresponding smoothed spectrum is also shown. For the remaining recordings only the smoothed spectra are shown. The spectrum in general shows a hump at 1–5 Hz band, falling off both at the lower as well as at the higher frequencies. The spectra for Bhatwari and Uttarkashi show a maximum in the frequency range of 2 to 4 Hz. The amplitudes fall at higher frequencies. The spectra for the *T* horizontal components at Bhatwari and Uttarkashi are richer in lower frequencies than the *L* horizontal as well as the vertical components. There is more energy in the higher frequencies in the horizontal components at Uttarkashi than at Bhatwari. This is consistent with the higher peak horizontal acceleration, a mainly high frequency phenomenon, observed at Uttarkashi.

The spectra at Ghansiali, Tehri and Koteshwar have relatively larger energy in the 0.6–0.9 Hz frequency range. The Tehri horizontal components are depleted in higher frequencies. The spectra at Rudraprayag have a peak at around 8 Hz indicative of resonance observed in the accelerogram. Similarly the horizontal components at Srinagar have a peak at this frequency. The Srinagar vertical also shows a hump in the 0.5–0.9 Hz range, corresponding to the distinct low frequency pulse in the

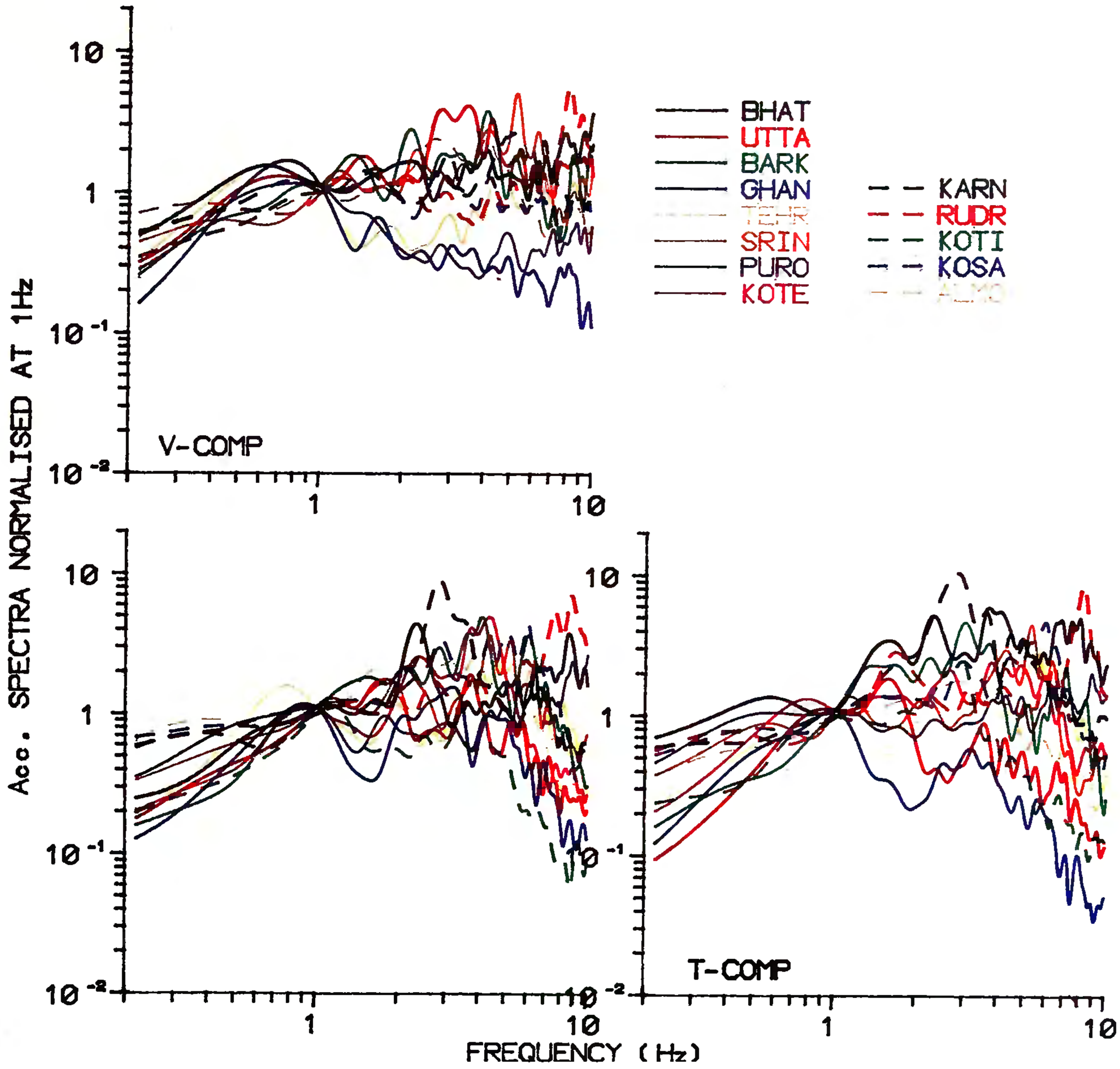

Figure 5. Fourier spectra of the observed accelerograms normalized at 1 Hz.

corresponding accelerogram. The horizontal components have a peak around 2–3 Hz corresponding to the resonance seen in the accelerograms. The vertical component is relatively flatter, with enrichment in the 4–6 Hz band. The spectra at Kosani and Almora have similar structure up to about 2 Hz, with departures seen at the higher frequencies.

In order to compare the relative distributions of the energy in various frequencies at different sites, the spectra normalized at 1 Hz are plotted in Figure 5. The station nearest to the fault at Bhatwari is rich in frequencies less than 1 Hz in the horizontal components. The stations at Uttarkashi and Ghansiali which are 10 to 25 km respectively from the rupture zone, show a faster decay of spectral amplitude for frequencies higher than 1 Hz. Tehri shows a maximum around 0.8 Hz in both the horizontal and the vertical components. Barkot which is at a distance of 20 km from the fault in the direction of rupture is poor in frequencies less than 1 Hz and rich in high frequencies. Thus the spectra in general is dominated by the local site effects rather than the directionality of the fault rupture and other source conditions.

Source spectrum

The spectra at Bhatwari and Uttarkashi, which are at distances very close to the edge of the fault, may be used to estimate the source spectrum. The average source spectrum obtained in this way is shown in Figure 6. This represents the spectrum at the surface and will

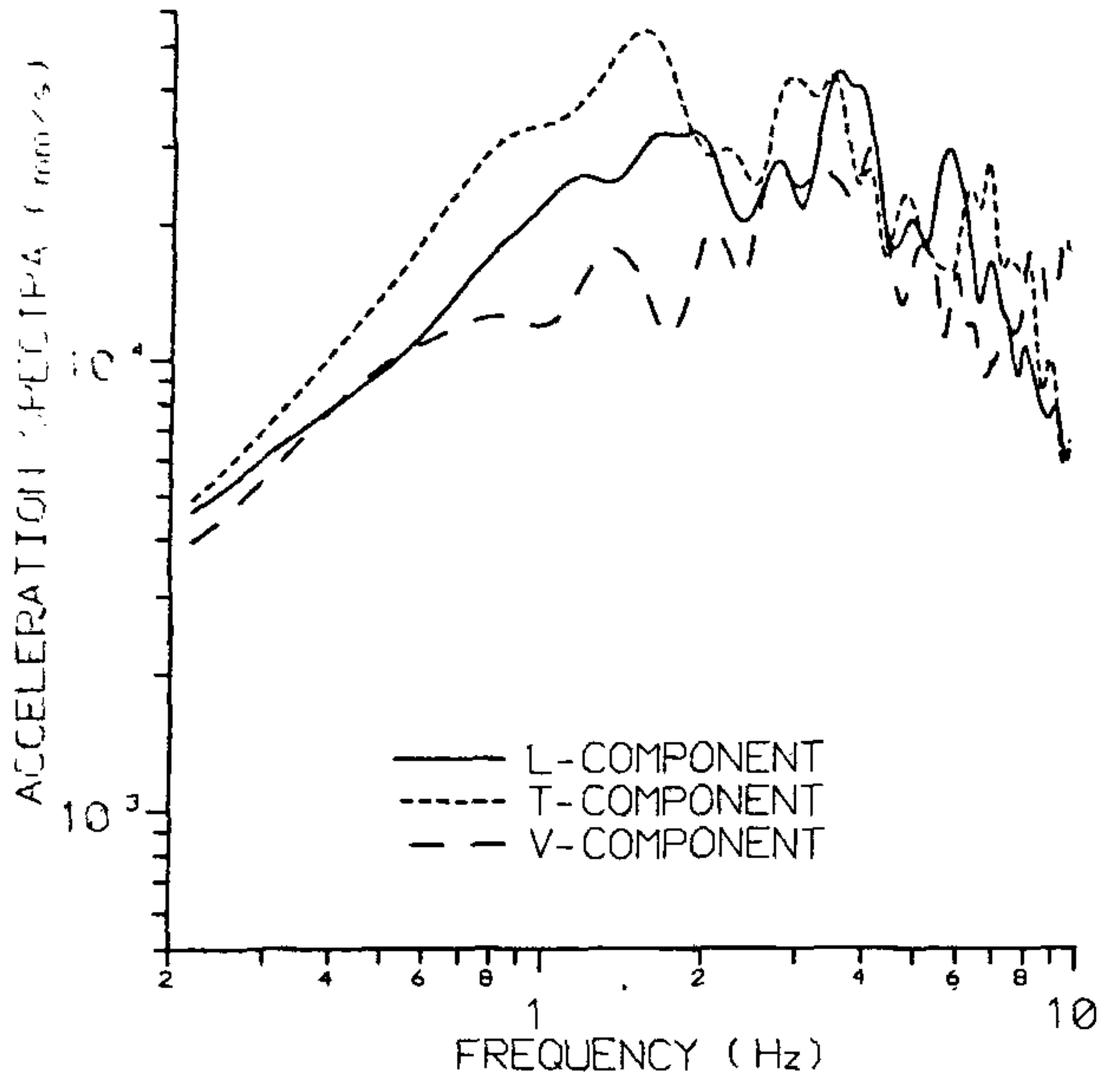

Figure 6. Average acceleration Fourier spectra to represent the 'source spectrum'.

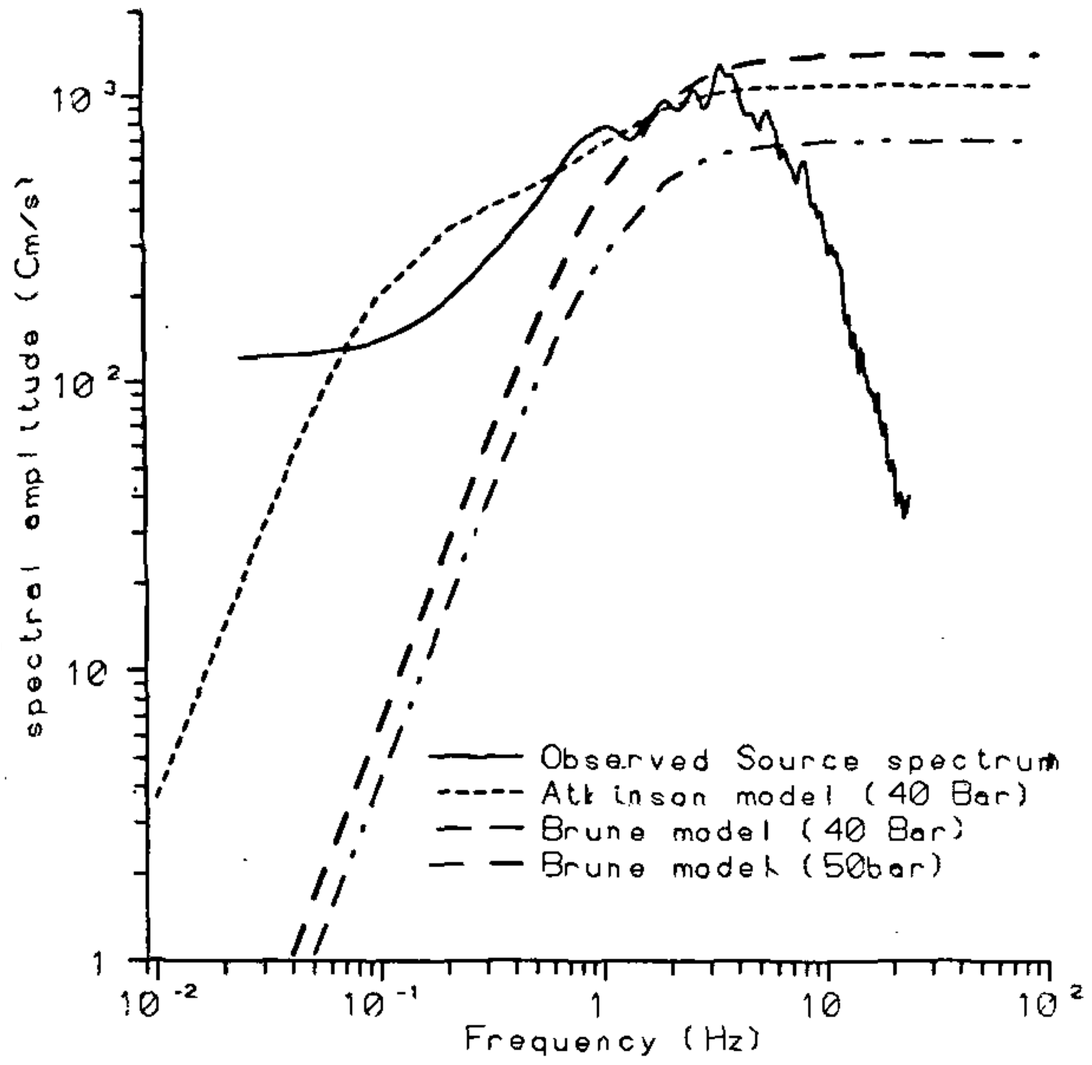

Figure 7. Observed source acceleration spectrum and the corresponding two Brune spectra composite model and the simple Brune model.

suffer from attenuation in the medium due to propagation. The corner frequency is expected to be at about 0.08 Hz and is outside the pass band of the accelerograms and so cannot been seen. On the other hand, we notice a corner at about 1 Hz. The source spectra of many earthquakes have been found to be characterized with a high frequency level with an attendant corner frequency and a low frequency level and corner frequency related with the moment of the earthquake. The spectra at the high frequencies is related to the roughness of the faulting process. Whereas the long period level and the lower corner frequency are related to the main smooth source[15]. The heterogeneous nature of faulting represented by the above character of the source spectrum has been modeled by multiple events[16,17], the specific barrier model[18], the asperity model[19,20] and the partial stress model[21]. More near-source earthquake records will be needed for establishing it. In the Brune model[21] commonly adopted for representing the source spectrum the high frequency level is governed by the stress drop and the low frequency level is proportional to the seismic moment. The spectrum here departs from the basic Brune model. The spectrum is depleted in intermediate frequencies. We do not know whether the observed depletion in the middle frequencies noticed in the Uttarkashi earthquakes is typical of the region. This may be due to the reasons mentioned above and also due to the model assuming a circular fault shape whereas in reality it may be rectangular or irregular in shape[22–24]. Atkinson[15] has found that such spectra for the horizontal component can be adequately modeled as a superposition of two Brune spectra having the following form.

$$A(f) = C(2\pi f)^2 M_o\{(1-\varepsilon)/[1+(f/f_{o2})^2] + \varepsilon/[1 + (f/f_{o1})^2]\},$$

where $C = R\pi FV/(4\pi\rho\beta^3 R)$ with $R = 1$ km, R_p average radiation pattern (= 0.55), F = free-surface amplification (= 2.0), V = partition of two horizontal components (= 0.71), ρ = the crustal density (= 0.28 g/cc), β = shear wave velocity (= 3.5 km/s) and ε is the moment partitioning parameter ($\log \varepsilon = 2.52–0.637\,M$ with M = magnitude). f_{o1} is the upper corner frequency and f_{o2} is the lower corner frequency. In the present case the lower corner frequency is estimated on the basis of fault dimension from the aftershock data. The corresponding stress parameter is 31 bars. The higher corner frequency is at 1.3 Hz. From the roughness spectrum envelope, the stress parameter obtained is 40 bars. The corresponding two corner source model is also shown in the Figure 7. The match between the empirically estimated spectra and the model is satisfactory in the 0.4–4.0 Hz band. At higher frequencies the drop in the observed spectrum is due to the attenuation in the propagation and perhaps also due to source properties. Towards the lower frequencies the mismatch could be due to the filtering applied in the conversion of the analog data to the digital mode.

Site response functions

The relative site response functions have been estimated by finding the average spectra for groups of stations that

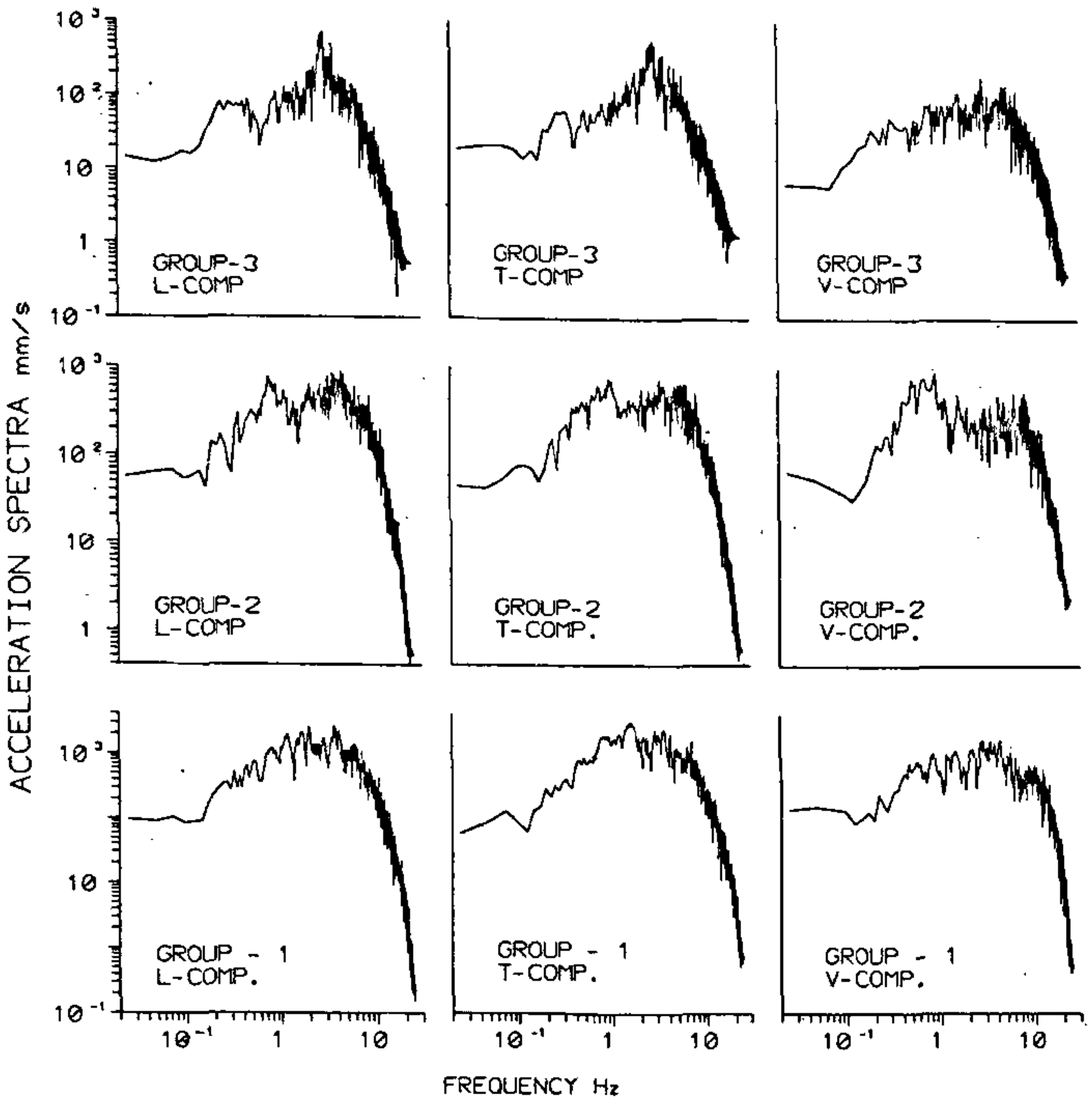

Figure 8. Average acceleration Fourier spectra for groups of stations. Group 1 stations, Bhatwari, Barkot, Uttarkashi, Purola and Koti; Group 2 stations, Ghansiali, Tehri, Koteshwar, Srinagar and Rudraprayag; Group 3 stations, Karanprayag, Kosani and Almora.

are at similar azimuth and distance from the fault edge. Three groups were formed and their average spectra are shown in Figure 8. One notices the consistency of the shape of the spectra. However, there is an enrichment in the frequency band of 0.5–1.0 Hz in the group of stations (including Tehri) on the SE of the fault plane. These average spectra were used to divide through the observed spectra at various stations to obtain estimates of the site amplification functions which are shown in Figure 9. The base line adopted for estimating the amplifications is the low frequency level in each function. In general the amplification bands are in the higher frequencies. We find that in most cases the amplifications are within a factor of 2 except at stations at Rudraprayag, Koteshwar and Karnaprayag where narrow band strong resonances at higher frequencies are present. However, at Tehri there is amplification by factors of about 1.5–2 in the middle frequency band of 0.4–1.0 Hz. This may be contributed by a shallow low velocity layer as well as by the topographic effects. Uttarkashi also shows an enrichment at higher frequencies.

The foregoing re-emphasizes the role of the local site conditions in significantly modifying the ground motions. Here, we see in particular, that the horizontal ground motions will be amplified by a factor of up to 2.5 in the band of frequencies that cover the natural frequencies of the Tehri dam, thus gravely enhancing the seismic hazard of the structure. This aspect has not been

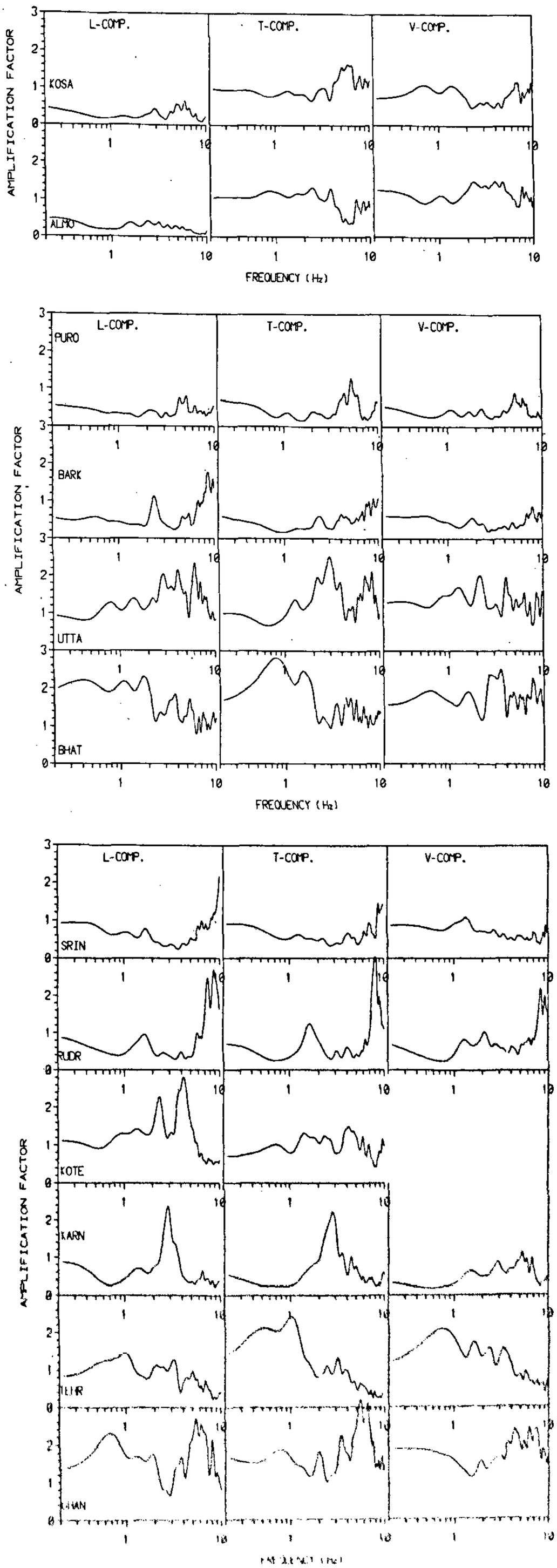

Figure 9. Site response spectra for the ground acceleration.

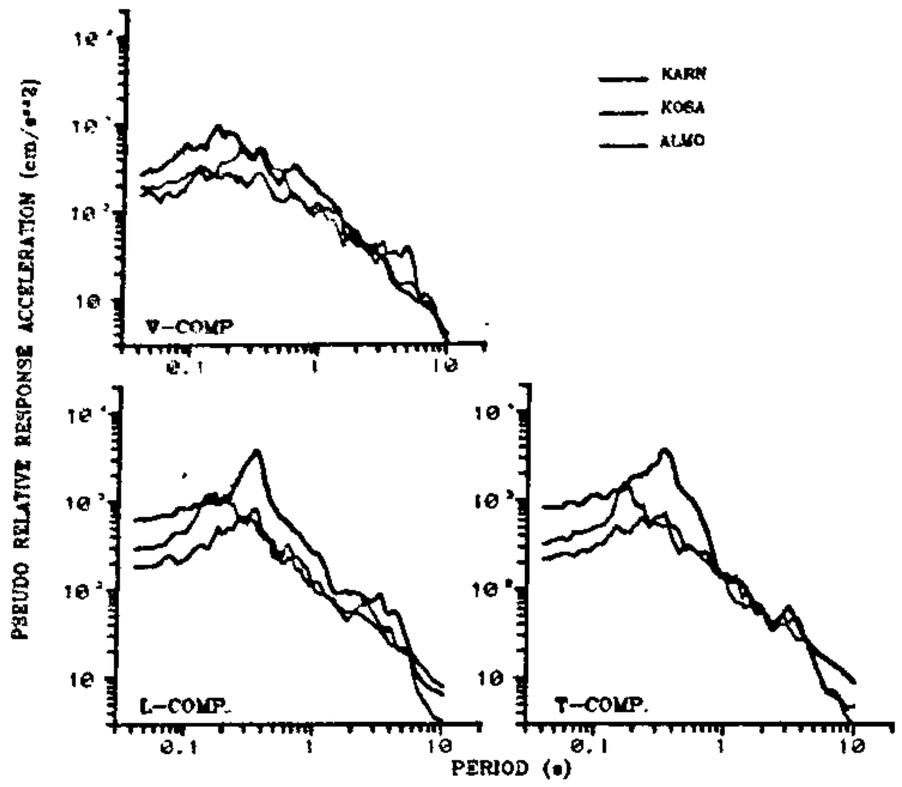

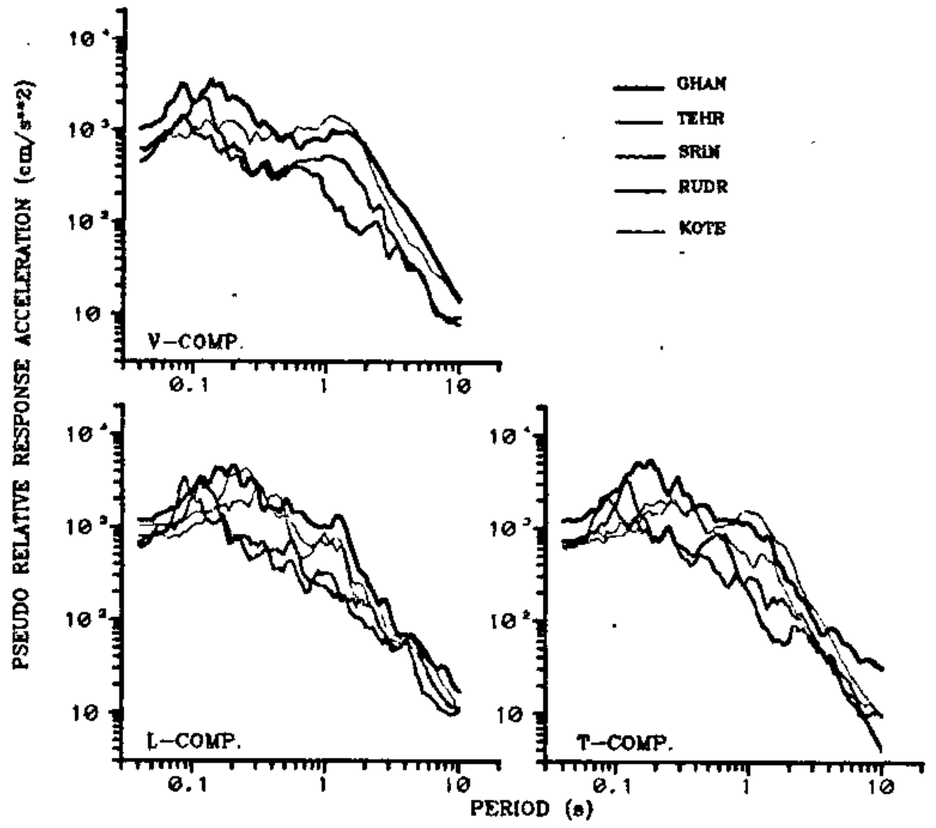

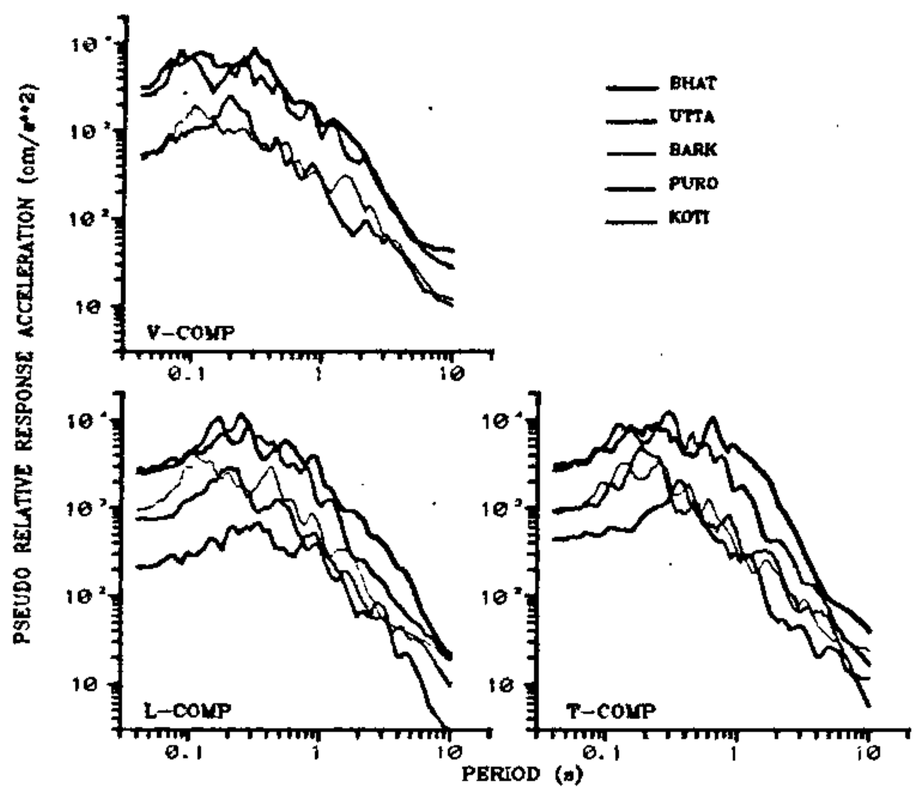

Figure 10. Response spectra for 5% damping for all the sites.

taken into account in the currently adopted design specifications of the dam.

Response spectrum

The response spectra (5% damping) for all the stations are shown in Figure 10. A comparison of the response spectra at Uttarkashi and Bhatwari shows that the amplitudes are considerably larger at longer periods at Bhatwari, whereas they tend to converge at periods shorter than about 0.6 s. Similarly, the response spectra for Tehri also show higher response values at periods longer than about 0.6 s. This is reflective of the dominance of longer periods in the accelerograms at these stations. Hence if we normalize the accelerograms from stations at various distances and average the corresponding response spectra to obtain an average response spectrum, we are going to get quite an inadequate picture for sites such as Tehri as the average response spectrum will be lacking the enhanced response at the longer periods.

To appreciate the extent of enrichment in the energy in the longer periods at Tehri and the nearby station at Ghansiali, their response spectra are shown in Figure 11 along with those of Bhatwari and Uttarkashi which are very near to the fault edge. The response spectra come closer together for all the four sites for periods greater than about 1 s for the vertical component while only Bhatwari is somewhat higher in the horizontal components. This shows the amplifying effect of the local geology at Tehri and Ghansiali. On the other hand, the response spectra diverge at shorter frequencies as is expected due to the attenuation effect of distance from the fault.

Attenuation of response spectrum with distance

The dependence of response spectrum on distance is shown in Figure 12. The dependence is plotted for four periods, that is 0.4, 0.75, 1.25 and 2.0 s. A significant

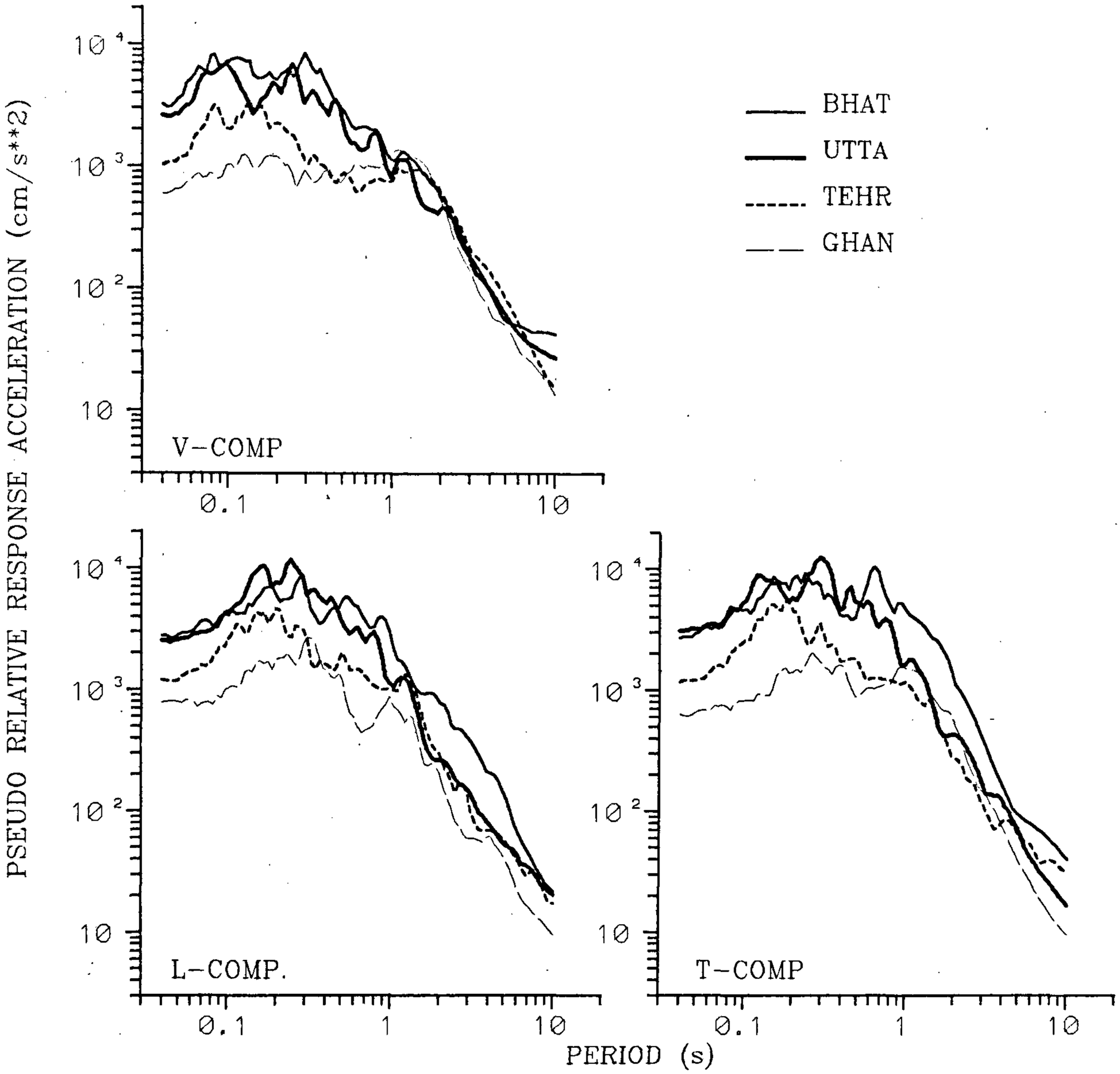

Figure 11. Comparison of the response spectra at Bhatwari, Uttarkashi, Tehri and Ghansiali.

observation is that the group of stations in the 40–50 km distance range generally show anamolously high amplitudes. The amplifications are more pronounced in the horizontal components and in the shorter periods. Tehri, Koteshwar, Ghansiali and Karnaprayag are among this group of stations. This phenomenon is a site characteristic. It may be further examined by investigating the local site geology, and by studying the relative amplitudes of the teleseismic signals.

Attenuation of Fourier spectrum with distance

The parameters required to model the attenuation of strong ground motion are numerous because of its random nature. But the major contributing factors are the hypocentral distance to the station and the anelasticity and the scattering of the medium. The spectral amplitudes of the strong ground motion at a distance R can thus be expressed as[25]

$$\log_{10} A(f, R) = \log_{10} A_0 - \gamma(f) \log_{10} R + (\pi f \log_{10}(e)/Q\beta)R + S(f),$$

where A_0 is the amplitude of the source spectrum, R is the epicentral distance, γ is the co-efficient of geometric spreading, f is frequency, Q is the shear wave quality factor and $S(f)$ is the site response.

At short distances (up to 100 km), multiply reflected or refracted waves reaching the station are less, and it can be safely assumed that the attenuation is proportional to $R^{-\gamma}$, where γ is the coefficient of geometric

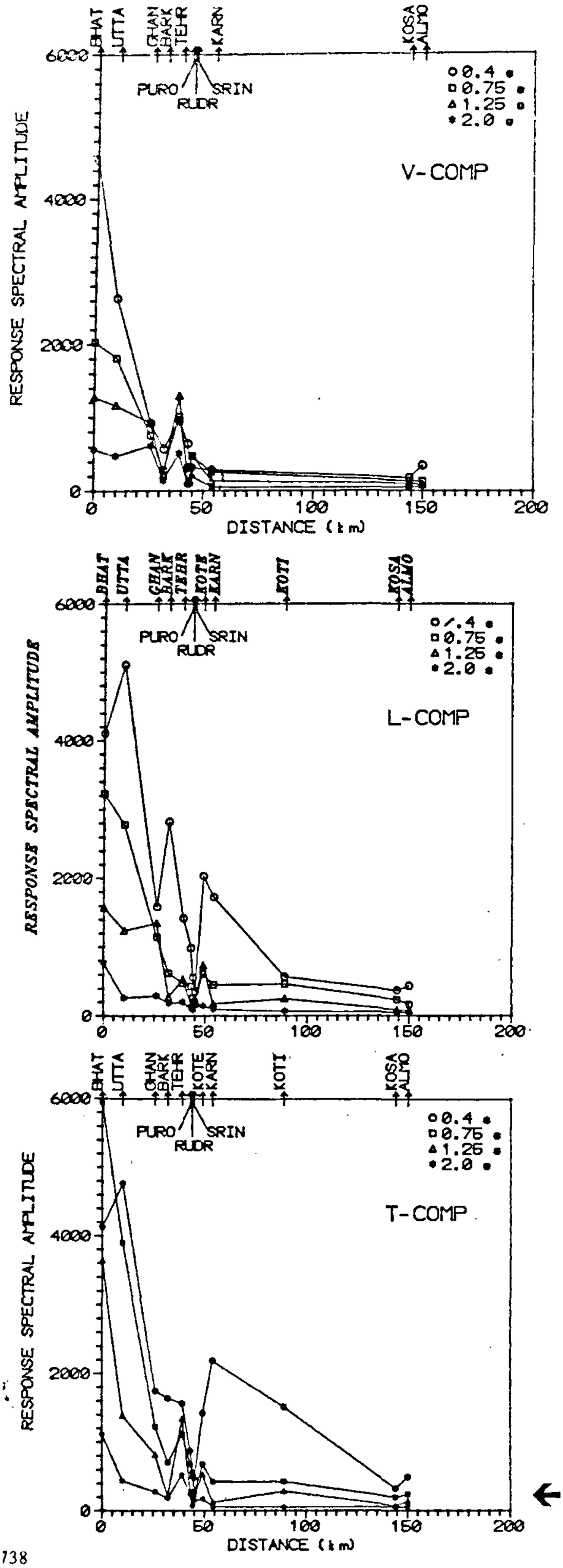

Figure 12. Decay of response spectra with distance for four periods.

spreading. The quality factor Q for the medium can be assumed to be constant, as for shallow earthquakes most of the wave energy is confined to the uppermost layer of the crust at short distances. A shear wave quality factor of 1000 is taken for this region based on the model given by Yu *et al.*[8].

The accelograms show that the shear phases are the most dominant in all the components and the P and its coda are weak. Hence the spectra from the whole accelerogram can be taken for the shear wave spectra. Using these assumptions, a regression is carried out for the coefficient of geometric spreading γ setting the site term to zero. The geometric spreading co-efficient is allowed to take different values for different distances and frequencies. The mean γ value thus obtained, need not be a true representative of the geometric spreading in the region, since it has accommodated the inadequacies in the assumption made for the regression. Using the value of γ in the above expression, the amplitude spectra are computed for all the stations. The differences between the observed and the computed spectra are taken as site responses. In Figure 13 the site responses thus obtained are shown for 5 stations in the distance range of 25 km from the source. Though the shape of the response matches with the response obtained from the spectral averaging method, the amplitude of the response in this method is larger by a factor of 2.5 or 3 in some cases.

The source spectrum and the site response function from the regression are used to normalize the observed spectral amplitudes to a common level in order to visualize the path effect. The variation of the normalized spectral amplitudes with distance for three different frequencies and for three components is shown in Figure 14. The data set is clustered in the distance range of up to 50 km. Only 2 points are available at about 150 km. Thus the results are better constrained for the shorter distance range. In this range the decay rates for all the three frequencies are the same within the resolution available. At larger distances there is a departure and the higher frequencies begin to show larger attenuation rates in a consistent manner.

Response spectrum and structural response records

A number of structural response recorders (SRRs) having natural periods 0.4 s, 0.75 s and 1.25 s are in operation throughout the country. At three locations, both the SRRs and the accelerographs have recorded the peak ground motions. A comparison of the readings at three periods 0.4 s, 0.75 s and 1.25 s for four stations is shown in Figure 15. While the values are comparable at

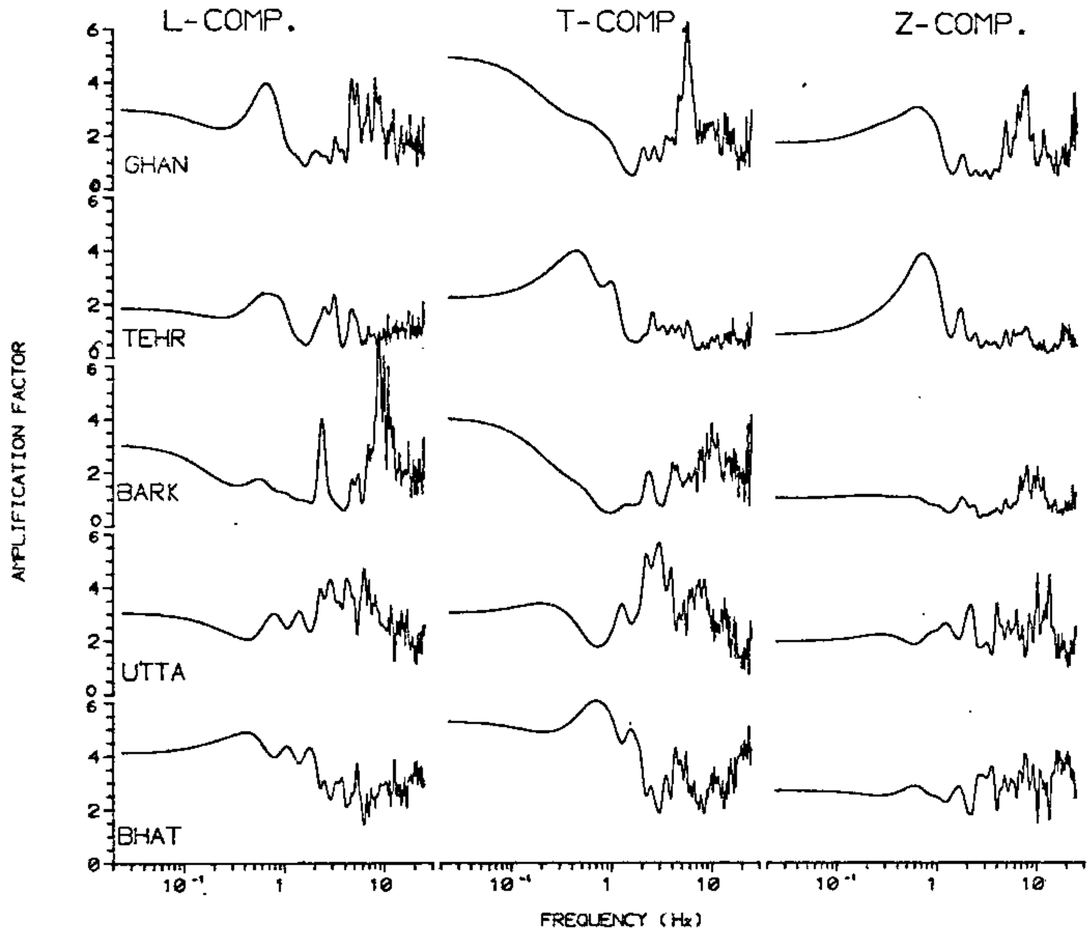

Figure 13. Site response functions obtained using regression technique (see text).

Bhatwari and Tehri, at the other two sites the SRRs values are considerably lower than the accelerograph values. At Uttarkashi, the SRRs values are proportionally lower at all periods. At Barkot, values are comparable at 0.4 s and 1.25 s while at 0.75 SRR give abnormally high value. This opens up the question of the fidelity of the SRRs.

Conclusions

The strong motion data for the Uttarkashi earthquake shows that the source spectrum for this earthquake is complex and may be represented by the superposition of two Brune spectra, one corresponding to the smooth slip over the whole fault plane and the other due to the roughness of fracturing over the fault plane corresponding to asperities and barriers. The corresponding stress parameters are 40 and 31 bars. The sites in the distance range of 40–50 km show significant amplification of response spectra. The sites at Tehri and Bhatwari show a considerable enrichment of low frequencies. Some sites

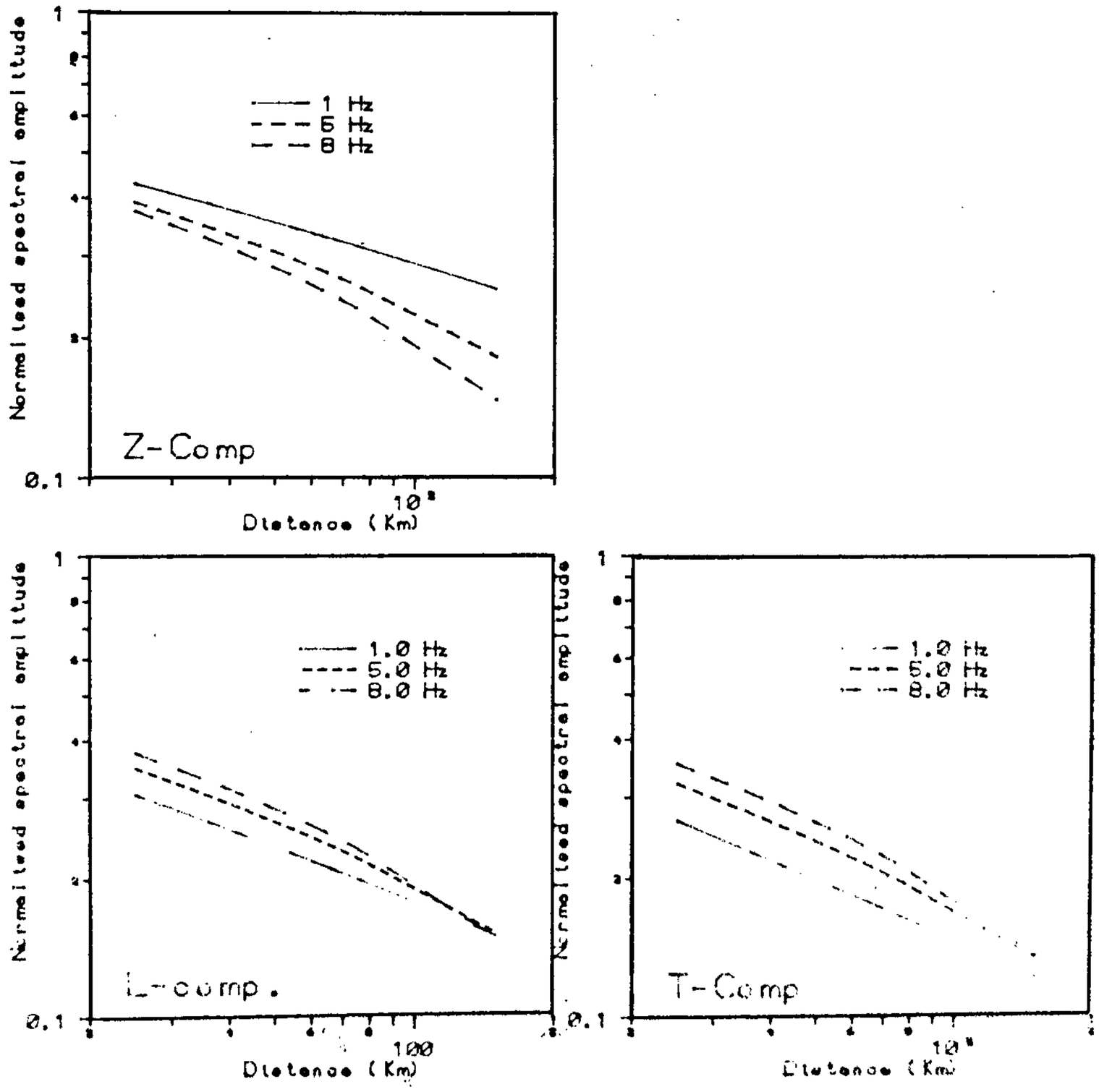

Figure 14. Dependence of the acceleration Fourier spectra on distance at three frequencies.

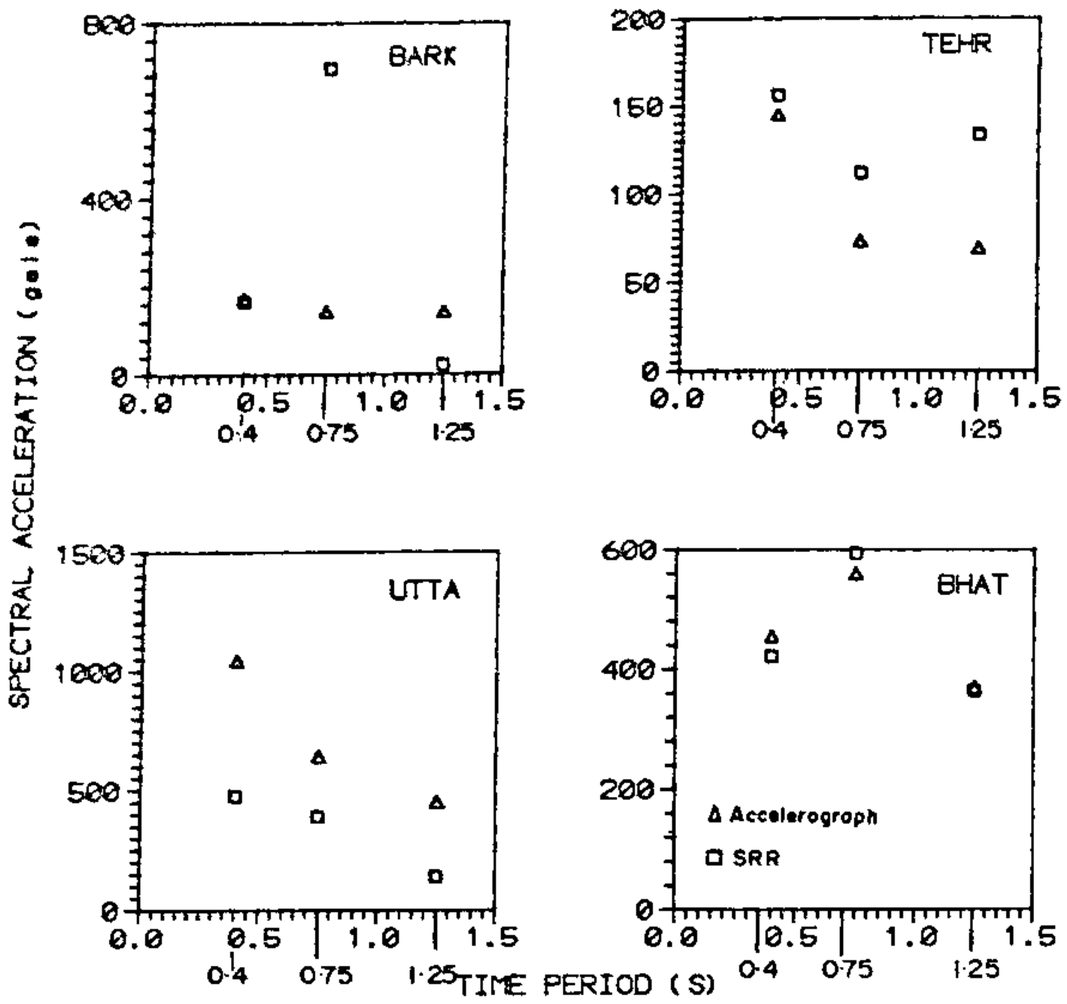

Figure 15. Comparison of the peak accelerations recorded using accelerographs and structural response recorders at the same sites.

show resonant narrow frequency bands towards the higher frequencies. The estimates of site amplification functions show amplifications in some frequency bands by factors of up to about 3. The amplification function at Tehri shows significant amplification by a factor of 2.5 in the period range of 1.0–2.5 s. The response spectra show site-specific characteristics. At Tehri there is a significantly larger response at longer periods (~1–2 s). These results show that assigning an average response spectrum for the purpose of earthquake-safe design of critical structures at such sites is not an adequate procedure. The attenuation of spectral ground acceleration with distance shows two distinct sections. For distances less than 60 km the attenuation is constant at all frequencies and for distances greater than 60 km the fall is more rapid for the higher frequency waves. The dependence of the peak ground acceleration on distance is better described by the relation based on the European data set[13] for the distances larger than 50 km while the relation based on the data set from Himalayan earthquakes[14] is better for the distance between 30 and 50 km.

1. Arya, A. S., *Mem. Geol. Soc. India*, 1995, **30**, 199–201.
2. Khattri, K. N., *Tectonophysics*, 1987, **138**, 79–92.
3. De Mets, C., Gordon, R. G., Argus, D. F. and Stein, S., *Geophys. J. Int.*, 1990, **101**, 425–475.
4. Seebar, L. and Armbruster, J. G., in *Earthquake Prediction, An International Review*, Marice Ewing Series, 4, Am. Geophys. Union, Washington, DC, 1984, pp. 259–277.
5. Khattri, K. N. and Tyagi, A. K., *Tectonophysics*, 1983, **96**, 281–297.
6. Middlemiss, C. S., *Mem. Geol. Surv. India*, 1980, **XXXVII**, 1–409.
7. Khattri, K. N., Zeng, Y., Anderson, J. G. and Brune, J., *J. Him. Geol.*, 1994, **5**, 161–191.
8. Yu, G., Khattri, K. N., Anderson, J. G., Brune, J. and Zeng, Y., *Bull. Seismol. Soc. Am.*, 1995, **85**, 31–50.
9. Atkinson, G. M. and Meeru, R. F., *Bull. Seismol. Soc. Am.*, 1992, **82**, 2014–2031.
10. Brijesh Chandra, Ashok Kumar, and Bansal, M. K., Memoir 30, Geological Society of India, Bangalore, 1995.
11. McGuire, R. K., *J. Geotech. Engg. Divn., ASCE*, 1978, **104**, 481–490.
12. Ambraseys, N. N., *Earthquake Engg. Struct. Dynam.*, 1995, **24**, 467–490.
13. Abrahamson, N. A. and Liteisher, J. J., *Bull. Soc. Am.*, 1989, **79**, 549–579.
14. Ashutosh Aman, Singh, U. K. and Singh, R. P., *Curr. Sci.*, 1995, **69**, 772–777.
15. Atkinson, G. M., *Bull. Seismol. Soc. Am.*, 1980, **70**, 1–28.
16. Joyner, W. B. and Boore, J. M., Proceedings of the Earthquake Engineering and Soil Dynamics, ASCE, Park City, Utah, 1988, pp. 33–102.
17. Boatwright, J., *Bull. Seismol. Soc. Am.*, 1980, **70**, 1–28.
18. Papageorgiou, A. and Aki, K., *Bull. Seismol. Soc. Am.*, 1983, **73**, 693–722.
19. Hartzell, S. and Brune, J., *Bull. Seismol. Soc. Am.*, 1979, **69**, 1166–1173.
20. McGarr, A., *J. Geophy. Res.*, 1981, **86**, 3901–3912.
21. Brune, J., *J. Geophys. Res.*, 1970, **75**, 4997–5009.
22. Haskell, N., *Bull. Seismol. Soc. Am.*, 1969, **59**, 865–908.
23. Savage, J., *J. Geophys. Res.*, 1972, **77**, 3788–3795.
24. Hadden, R., *Bull. Seismol. Soc. Am.*, 1992, **82**, 720–754.
25. Knopoff, L., *Rev. Geophys.*, 1964, **2**, 625–660.

ACKNOWLEDGEMENTS. K.N.K. thanks CSIR for the support of this work under an ES scheme. We also acknowledge the WIHG for promoting this investigation. Prof. J. G. Anderson offered useful suggestions.

Received 12 December 1996; accepted 1 March 1997